Physical Interaction via Dynamic Primitives

Neville Hogan

Abstract Humans out-perform contemporary robots despite vastly slower 'wetware' (e.g. neurons) and 'hardware' (e.g. muscles). The basis of human sensory-motor performance appears to be quite different from that of robots. Human haptic perception is not compatible with Riemannian geometry, the foundation of classical mechanics and robot control. Instead, evidence suggests that human control is based on dynamic primitives, which enable highly dynamic behavior with minimal high-level supervision and intervention. Motion primitives include submovements (discrete actions) and oscillations (rhythmic behavior). Adding mechanical impedance as a class of dynamic primitives facilitates controlling physical interaction. Both motion and interaction primitives may be combined by re-purposing the classical equivalent electric circuit and extending it to a nonlinear equivalent network. It highlights the contrast between the dynamics of physical systems and the dynamics of computation and information processing. Choosing appropriate task-specific impedance may be cast as a stochastic optimization problem, though its solution remains challenging. The composability of dynamic primitives, including mechanical impedances, enables complex tasks, including multi-limb coordination, to be treated as a composite of simpler tasks, each represented by an equivalent network. The most useful form of nonlinear equivalent network requires the interactive dynamics to respond to deviations from the motion that would occur without interaction. That suggests some form of underlying geometric structure but which geometry is induced by a composition of motion and interactive dynamic primitives? Answering that question might pave the way to achieve superior robot control and seamless human-robot collaboration.

Keywords Tool use · Physical interaction · Dynamic primitives · Equivalent networks · Mechanical impedance

Submitted to: Laumond, J.-P. Geometric and Numerical Foundations of Movement.

N. Hogan (✉)
Department of Mechanical Engineering, Department of Brain and Cognitive Sciences,
Massachusetts Institute of Technology, 77 Massachusetts Avenue,
Room 3-146, Cambridge, MA 02139, USA
e-mail: neville@mit.edu

J.-P. Laumond et al. (eds.), *Geometric and Numerical Foundations of Movements*,
Springer Tracts in Advanced Robotics 117, DOI 10.1007/978-3-319-51547-2_12

1 The Paradox of Human Performance

Using tools is a hallmark of human behavior. While some animals have been shown capable of making and using tools, this ability remains the distinctive signature that has given humans an evolutionary advantage [10, 51, 53, 60]. Tool use requires dexterous control of physical interaction, and we excel at it. Yet one of the most critical features of the human neuromuscular system is that it is agonizingly slow. The fastest neural transmission speed in humans is no more than 120 m/s [56]. That compares very poorly with information transmission in electro-mechanical systems such as robots, which can conservatively be estimated at 10^8 m/s, about a million times faster. Moreover, muscles are slow. The typical isometric twitch contraction time[1] for the human biceps brachii is about 50 ms [56]. Assuming a linearized model to approximate this behavior implies a bandwidth of about 3 Hz. In comparison, electro-mechanical actuator technology routinely achieves bandwidths from tens to hundreds of Hz [9, 76, 84] and can achieve motion up to 1 KHz, albeit in specialized applications [8, 77]. Furthermore, our brains are slow. A now-classical study of human mental rotations to assess congruency of visually-presented objects demonstrated a reaction time of about 1 second plus 1 additional second per 60° of rotation (i.e. ∼4 s for a 180° rotation) [96].

Despite slow neurons, muscles and brains, humans achieve astonishing agility and dexterity manipulating objects—and especially using tools—far superior to anything yet achieved in robotic systems. Slow neuro-mechanical response implies that *prediction* using some form of internal representation is a key aspect of human motor control, yet the nature of that representation remains unclear [18, 27, 57, 111]. Consider fly-casting or cracking a whip: These objects comprise flexible materials that interact with complex compressible fluid dynamics and, in the case of whip-cracking, operate into the hypersonic regime. Models of their behavior based on mechanical physics tax even modern super-computers. The likelihood that anything resembling a physics-based model underlies real-time human control of these objects seems slim, yet some humans can manipulate them with astonishing skill. If humans use internal models for planning and predictive control of dynamic objects—which seems likely—what form might their internal models take?

2 Human Performance Is Not Consistent with Riemannian Geometry

To address this question we studied *haptic illusions* [26]. 'Haptic' refers to the combination of motor and sensory information used when we feel objects, sometimes also called 'active touch'. 'Illusion' in this context refers to the fact that, like other perceptual modalities (e.g. vision), haptic perception is distorted. Experimentally, it

[1] Twitch contraction time is the time from an impulsive stimulus (e.g. electrical) to peak isometric tension.

is observed that the perceived length of a line segment depends on its orientation with respect to the subject; line segments oriented radially from the shoulder are perceived as being longer than line segments oriented tangentially to circles centered at the shoulder [63, 73]. Moreover, the amount of distortion is configuration dependent; distortion becomes more pronounced as the center of the object moves away from the shoulder [45].

During contact and physical interaction, afferent and efferent information is acquired. Afferent information comes from mechanoreceptors such as cutaneous and deep tissue sensors, muscle spindles, Golgi tendon organs and joint capsule receptors [56]. Efferent information is available from so-called corollary discharge, information available from motor areas of the central nervous system (CNS) that project onto sensory areas [56]. Percepts of external objects are formed based on afferent and efferent information acquired during interaction. Perception of objects can be viewed as an integrative, computational process in which geometric properties are inferred from acquired efferent and/or afferent information, combined with prior knowledge. Geometric properties of objects, such as lengths of segments, continuity of paths, angles between edges, etc., may be determined based on the spatial stimulus alone. It therefore seems reasonable to describe the perceptual processes as implementing an underlying, abstract geometrical reasoning system.

What geometric structure underlies human sensory-motor performance? A distorted haptic perception might reflect a Riemannian geometry, consistent with classical mechanics. Riemannian geometry is a mathematically simple extension of Euclidean geometry based on an inner product of vectors v and w denoted $\langle v, w\rangle = v^T G w$, where the metric G is characterized by a symmetric, positive-definite matrix. This metric can vary from location to location and, in general, haptic perceptual distortion is known to be location dependent [45]. In our study we were concerned only with haptic perceptual distortion in a small region, hence we assumed the metric was effectively constant.

Inner products provide measures of length and measures of angle. The length of a vector v is the square root of the inner product of that vector with itself, $\|v\| = \langle v, v\rangle^{1/2}$. The angle α between two vectors v and w may be determined from $\langle v, w\rangle = \|v\|\|w\| \cos\alpha$. To be metrically consistent, the perception of length and angle must be related. If the metric is constant in a given locality (as we assumed) the Riemannian geometry corresponds to a linear stretch of Euclidean geometry (Fig. 1). If, due to perceptual distortion, a certain rectangle is perceived to be square, then if that rectangle is cut in half along the diagonal, a metrically consistent observer would perceive the acute angles of the resulting right triangle to be equal.

To test the metric consistency of human haptic perception, we measured subjects' judgment of length and angle at the same workspace location; details are in [26]. In a length-judgment experiment, subjects felt rectangular holes oriented at 0° and 45° (the latter shown schematically in Fig. 2, Panel (a) and judged which pair of sides was longer. The rectangular holes were simulated by a planar robotic manipulandum with two degrees of freedom. Rectangles of the same area but with 15 different aspect ratios were presented, allowing accurate assessment of the rectangle which

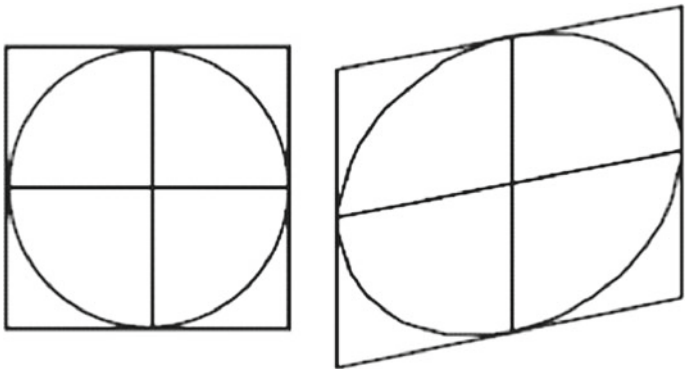

Fig. 1 With a constant metric, a Riemannian geometry is a linear stretch of a Euclidean geometry. Reproduced from [26]

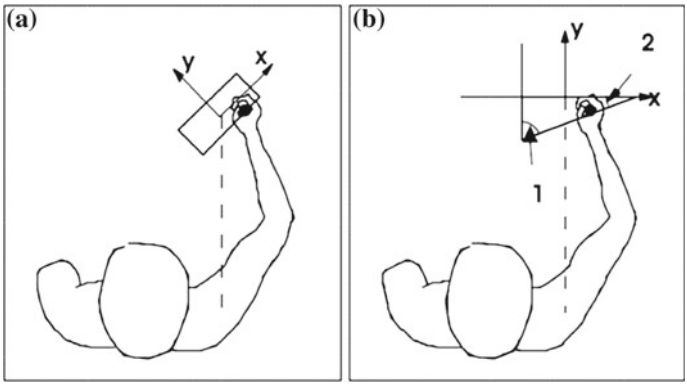

Fig. 2 Panel **a** Subjects felt rectangular holes and were asked to judge which sides were longer. Panel **b** Subjects felt triangular holes and were asked to judge which acute angle was larger. Reproduced from [26]

was perceived to be square. That information for the two orientations was sufficient to identify a metric underlying haptic length perception.

A metric can be used to generate geometrical shapes similar to Euclidean shapes. For example, a Riemannian circle of radius r can be identified with the set of displacement vectors of length r from its center, $\{v | v^T G v = r\}$. This is the equation of an ellipse which can be used to depict the 'subjective circle' corresponding to haptic length perception. The 'subjective circles' for 8 subjects were remarkably similar, with an eccentricity of $\epsilon = 1.29$ and a major axis oriented at $\theta = 17°$ counterclockwise from the line joining the shoulders (Fig. 3, Panel a).

In an angle-judgment experiment at the same location, subjects felt triangular holes oriented at 0° and 45° (the former shown schematically in Fig. 2, Panel b) and judged which acute angle was larger. To prevent inference based on judging

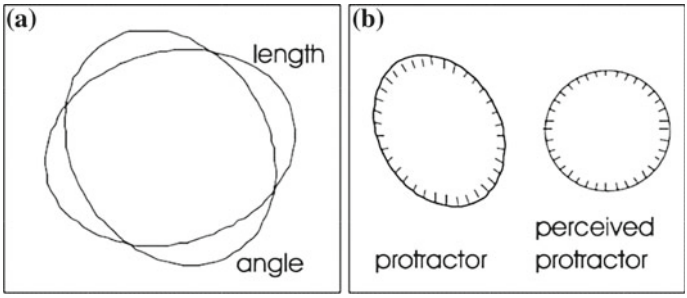

Fig. 3 **Panel a** Average subjective circles determined from the length experiment ($\epsilon = 1.29, \theta = 17°$) and the angle experiment ($\epsilon = 1.28, \theta = -62°$). **Panel b** The angle judgment experiment implies the observer uses the distorted protractor shown on the *left*, which is perceived as the Euclidean protractor on the *right*. Reproduced from [26]

the lengths of the perpendicular sides, the right-angled corner was inaccessible (see [26] for details). Triangles with a constant base length and 19 different aspect ratios were presented, allowing accurate assessment of the angles that were perceived to be equal. That information for the two orientations was sufficient to identify a metric underlying haptic angle perception. The 'subjective circles' corresponding to haptic angle perception were more variable between subjects but had an average eccentricity of 1.28 and a major axis oriented at –62° counter-clockwise from the line joining the shoulders (Fig. 3, Panel a). This difference was highly significant ($p < 0.01$).

This is remarkable. Riemannian geometry is a foundation of mechanical physics. Yet, at least in the context of haptic perception, the brain's 'internal representation' is not consistent with Riemannian geometry.

3 Dynamic Primitives

Combined with the slow response of muscles, the long communication delays due to slow neural transmission impair reactive control. It therefore appears that a major component of human motor control requires planning and 'pre-computation' using some internal representation of the relevant dynamics. Neural evidence has been presented to support this hypothesis, and suggests that the cerebellum is one of the major structures instantiating this 'internal model' [7, 111]. Prediction based on the mathematical models of mechanical physics figures prominently in the control of modern robots yet it appears that our 'internal models' are incompatible with those of mechanical physics—even the underlying geometry is incompatible. Nevertheless, humans substantially out-perform robots. What might be alternative bases for our internal models?

One possibility is that human motor performance is based on dynamic primitives [47, 48, 52]. A dynamic primitive is conceived as an attractor that emerges from

the nonlinear dynamics of a neuro-mechanical system—a network of neurons and/or their interaction with the musculo-skeletal periphery [20, 52, 97, 102]. Examples include the familiar point attractor (which may underlie the maintenance of posture) and limit-cycle attractor (which may give rise to rhythmic behavior). Attractor dynamics confers important stability and robustness. It also accounts for nonlinear interference between primitives [19, 94, 100, 101]. Evoking or 'launching' a dynamic primitive may require minimal central control and reduce the need for continuous intervention. At the same time, because each primitive is a highly dynamic behavior, highly dynamic performance may be achieved.

4 Evidence of Dynamic Primitives

Biological evidence supports this account. The most compelling comes from observations of persons recovering their ability to move after having survived a stroke (cerebral vascular accident) that left them partially paralyzed. In the course of studying the feasibility and effectiveness of using physically-interactive robots to aid neuro-recovery, kinematic records were obtained of the earliest movements made by patients as they recovered [61]. These first recovered movements were conspicuously fragmented. Even simple point-to-point reaching movements exhibited a highly irregular speed profile, with large speed fluctuations and frequent stops. This is quite unlike unimpaired movements, which tend to be smooth [29].

Remarkably, each of the movement fragments exhibited a highly stereotyped speed profile—even for patients with brain lesions of widely differing location and extent [61]. This suggests that human movements are composed of primitive submovements. A submovement may be defined as an attractor that describes a smooth sigmoidal transition of a variable from one value to another with a stereotyped time profile [47]. For limb position, the variable is a vector in some coordinate frame, e.g., hand position in visually-relevant coordinates $\mathbf{x} = [x_1, x_2 \ldots x_n]^T$. Each coordinate's speed profile has the same unimodal shape which has finite support: $\dot{x}_j(t) = \hat{v}_j \sigma(t)\,,\ j = 1 \ldots n$ where $\hat{v}_j$ is the peak speed of the submovement; $\sigma(t) > 0$ iff $b < t < e$ where b is the time when the submovement begins and e is the time it ends, otherwise $\sigma(t) = 0$; and the speed profile has only one peak: there is only one point $t_p \in (b, e)$ at which $\dot{\sigma}\left(t_p\right) = 0$ and at that point $\sigma\left(t_p\right) = 1$. This definition was used to identify sequences of submovements underlying continuous movements.

Reliably extracting overlapping submovements from a continuous kinematic record is a notoriously hard problem. The common practice of examining zero-crossings of progressively higher derivatives (acceleration, jerk, etc.) is fundamentally misleading. Even aside from the practical difficulty of obtaining reliable higher-order derivatives from kinematic data, a composition of two single-peaked speed profiles may yield a composite speed profile with one, two or three speed peaks, hence one to five zero-crossings in the acceleration profile, etc. [92]. Instead, submovement identification is better approached as an optimization problem, minimizing

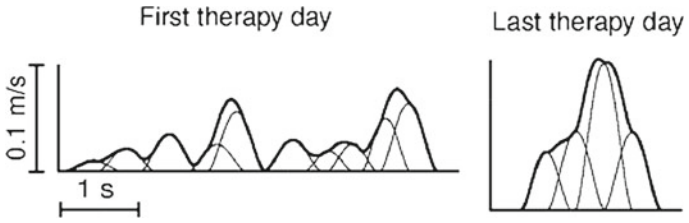

Fig. 4 Typical movements of one representative patient on the first and last therapy days. *Bold lines* indicate tangential speed measured during movement. The later movement is briefer with a single speed peak, while the earlier movement has an irregular speed profile with multiple peaks. Fine lines indicate underlying submovements. The later movement shows fewer submovements which have greater peak speed, duration and overlap than the earlier movement. Reproduced from [91]

mean-squared error between kinematic data and its reconstruction as a sequence of submovements. That avoids the problems mentioned above and yields robust identification even in the presence of substantial measurement noise [92, 93].

This approach was applied to identify submovement sequences in the movements of a cohort of 41 sub-acute and chronic phase stroke survivors as they progressed through robot-aided therapy [91]. Although there was substantial variability across patients, who had widely differing brain lesions, as they recovered they made fewer submovements, which had higher peak speed, longer duration and greater temporal overlap; these changes were statistically significant ($p < 0.05$). Figure 4 shows typical submovements of one patient observed on the first and last days of therapy. These observations indicate that the ability to generate stereotyped submovements appears to be preserved after injury to the CNS and that a major part of the recovery process manifests as re-learning how to combine and blend these dynamic primitives to produce desired behavior.

5 Consequences of Control via Dynamic Primitives

Motor control based on dynamic primitives may facilitate performance of highly dynamic behavior without the need for continuous intervention by the higher levels of the CNS. However, it may also lead to limitations of motor performance that cannot be ascribed to biomechanics. In particular, the parameters of submovements appear to be limited. Their maximum duration is typically on the order of a second. There appears to be a 'refractory period', a minimum interval (on the order of 100 ms) between the onsets of adjacent submovements. Together, these limitations imply that humans would have difficulty generating slow, smooth movements. Observations of unimpaired human subjects have confirmed this prediction. In one experiment, unimpaired subjects made horizontal planar discrete reaching movements between two targets 14 cm apart in the mid-sagittal plane. Subjects were instructed to move smoothly at three different self-paced speeds: 'comfortable', 'fast' (instructed to be

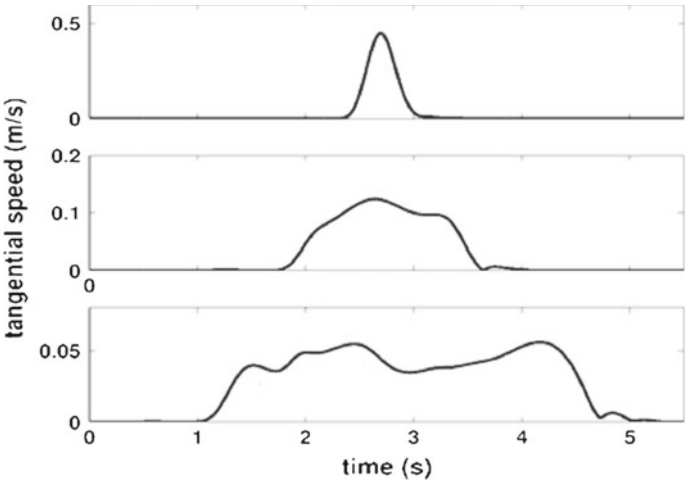

Fig. 5 Tangential speed profiles of discrete reaching movements made by an unimpaired subject at three self-paced speeds. *Top* 'fast'; middle: 'comfortable'; *Bottom* 'slow'. Note the different vertical scales. Slower movements were progressively more irregular

twice as fast as 'comfortable') and 'slow' (instructed to be twice as slow as 'comfortable'). Averaged across subjects, peak speeds were 0.28 ± 0.04 m/s (mean $\pm$ standard deviation) for 'fast' movements; 0.10 ± 0.03m/s for 'comfortable' movements; and 0.05 ± 0.01m/s for 'slow' movements, demonstrating that subjects could successfully follow task instructions.

Figure 5 shows typical speed profiles for the three cases. The 'fast' movement has a single speed peak with a 'bell-shaped' profile similar to that of a maximally-smooth movement [29]. The speed profile of the 'comfortable' movement also has a single speed peak, but is noticeably more irregular. Irregularity of the speed profile is most pronounced in the 'slow' movement, which has multiple peaks. Figure 6 shows a different set of movements for the three cases, and includes the minimal sequences of overlapping submovements that fit the speed profiles with residual error less than 3%. Each submovement has a support-bounded lognormal speed profile, which may be lepto- or platy-kurtic and positively or negatively skewed [85]. With a statistical significance $p < 0.01$ the number of submovements increased with movement duration: $n_{slow} > n_{comfortable} > n_{fast}$.

Taken together, these data provide strong evidence that discrete reaching movements are composed of submovements. The observations of submovements in stroke patients as they recovered was serendipitous (they were not the focus of the experiments) but could not be overlooked. The observation that speed fluctuations increased as unimpaired subjects moved slowly cannot be attributed to mechanics or biomechanics. Factors that might contribute to movement irregularity, such as the torques required to compensate for nonlinear kinematic and inertial coupling between joints or the nonlinear and noisy behavior of muscles, all decline as movements slow. The

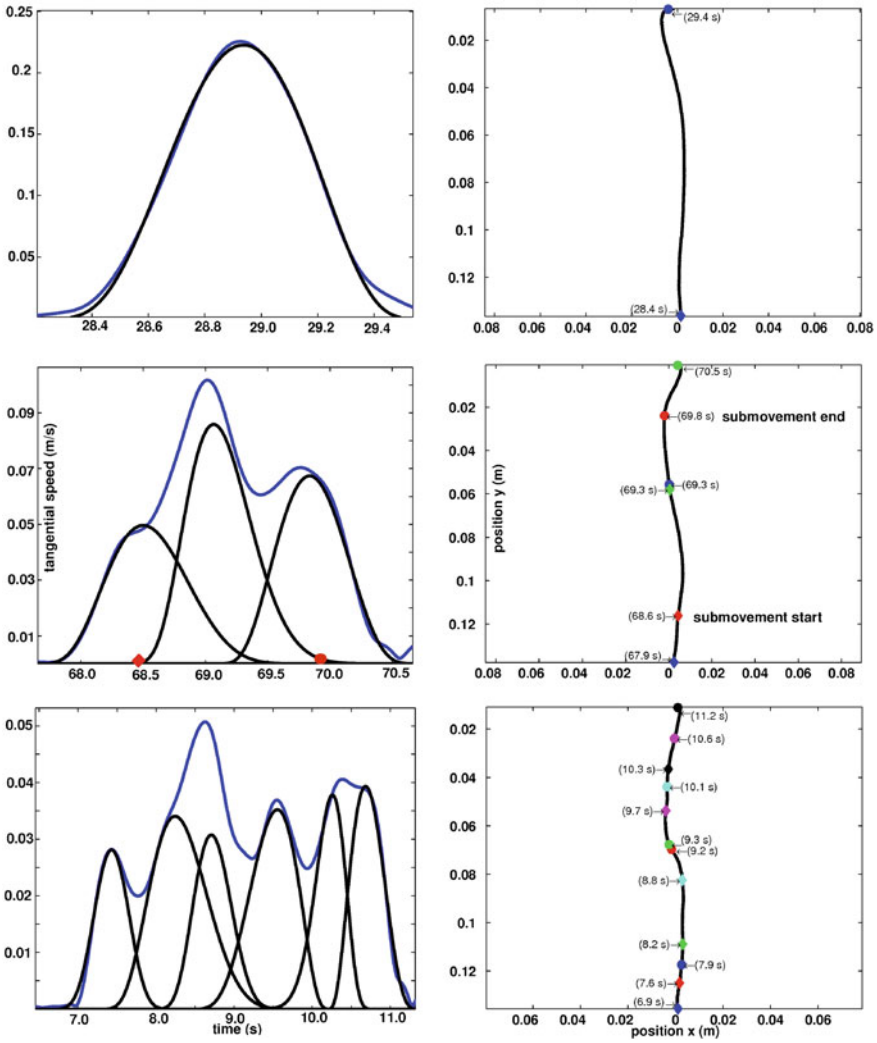

Fig. 6 Tangential speed profiles (*left*) and paths (*right*) of discrete reaching movements made by an unimpaired subject at three self-paced speeds: 'fast' (*top*); 'comfortable' (*middle*); 'slow' (*bottom*). The underlying sequences of submovements are superimposed. *Colored dots* denote the beginning and end of each submovement

fact that, instead, they increased strongly implicates the 'software' underlying motor control. Moving slowly and smoothly is hard for humans.

Similar results have been reported for rhythmic movements: unimpaired subjects were unable to sustain smoothly rhythmic performance as period increased; instead, kinematic irregularity increased as movement slowed, consistent with composition as a sequence of submovements [22, 23]. A complementary result was reported in

another study: unimpaired subjects made sequential back-and-forth discrete movements, instructed to dwell at rest at the end of each movement for a duration equal to the movement time. Movements were paced by a metronome which slowly decreased its period. As frequency increased, subjects were progressively less able to sustain the dwell at the end of movement, eventually producing smoothly rhythmic movements. Importantly, changing the duration of the metronome sound (to 50% of the metronome period) significantly reduced the frequency at which dwell time disappeared. In that case, the passage to zero dwell time cannot be attributed to biomechanical limitations, because with different sensory conditions subjects were demonstrably capable of faster discrete movements with non-zero dwell time. Instead, subjects switched to using an oscillatory dynamic primitive. This was confirmed by a 'discreteness index' which changed abruptly from values corresponding to discrete movements to those corresponding to smoothly rhythmic movements [103].

6 Dynamic Primitives for Physical Interaction

Submovements and oscillations may provide a basis for unconstrained movements, but contact and physical interaction are essential for that quintessentially human ability, manipulating objects and using tools. It may seem reasonable to control force when in contact with objects, but that is not sufficient. Simple hand tools illustrate this point; many are elaborated versions of a stick that you push on. A woodworker's chisel is a stick with a sharpened tip; axial compression is required to cut with it. A screwdriver is a stick with a specialized tip designed to mate with a corresponding shape in the head of a screw; to use it effectively, it must be maintained in axial compression.

Unfortunately, pushing on a stick destabilizes its posture. Consider a stick of length R pushed against a surface. To keep matters simple, assume its tip cannot slip but may pivot about the point of contact on the surface.[2] If the stick is initially perpendicular to the surface, the compressive force f_c exerted by the hand on the stick must be strictly axial, also perpendicular to the surface. Small angular displacements $\Delta\theta$ of the stick's orientation from the perpendicular (which might arise from fluctuations or "noise" in the neuromuscular system) displace the point of action of the force laterally (i.e. parallel to the surface) by an amount $\Delta x \cong R\Delta\theta$. If the force exerted by the hand is maintained constant in magnitude and direction, displacement evokes a torque about the tip of $\tau_{tip} = f_c \Delta x \cong (f_c R)\,\Delta\theta$ which acts to increase the deviation. Force control in this situation is statically unstable [89].

To counteract this effect the hand must generate the equivalent of a lateral translational stiffness k_{xx} at the point of contact with the tool so as to produce a lateral restoring force $f_x = -k_{xx}\Delta x$. This generates a rotational restoring torque $\tau = -\left(R^2 k_{xx}\right)\Delta\theta$ about the tip. The minimum stiffness required to maintain static

[2] This is one advantage of a Phillips (cross-head) screwdriver, invented by John P. Thompson, U.S. Patent 1,908,080 May 9, 1933, assigned to Henry F. Phillips.

stability is $k_{xx} > f_c/R$. This highly simplified analysis demonstrates a point that may easily be overlooked: even in this idealized *static* task (nothing varies with time) to exert a *force independent of motion would be unworkable*. Because the act of exerting force may destabilize posture, stiffness must also be present to ensure stability, and greater stiffness is required to stabilize greater forces. Humans generate the required stiffness via the grip of the fingers on the handle, supported by the wrist, the shoulder, and so forth. Remarkably, because the minimum required stiffness increases with applied force, the maximum force a human can exert in this task is determined by the limits of muscle-generated stiffness rather than by the limits of muscle-generated force [90].

Generating stiffness is a minimum requirement for controlling interaction. More generally, other effects equivalent to viscous damping and/or higher-order phenomena will also be required, collectively termed mechanical impedance. Loosely speaking, mechanical impedance is a generalization of stiffness to encompass nonlinear dynamic behavior [39, 44]. Mathematically, it is a dynamic operator that determines the force (time-history) evoked by an imposed displacement (time-history). Physical interaction requires including mechanical impedances as an additional class of dynamic primitives to describe force evoked by motion [47, 48]. Biologically, mechanical impedance at the hand may be modulated by adjusting neural reflex gains [37, 80], co-activating opposing muscles [38, 50], selecting the pose or configuration of the limbs [42] or combinations of these approaches.

The practicality of mechanical impedance as a dynamic primitive underlying human dexterity was demonstrated by implementing it in a 'bio-mimetic' controller for a motorized trans-humeral amputation prosthesis [2]. Control inputs were derived from surface myoelectric activity (EMG) obtained from antagonist muscles in the limb residuum. The difference of their amplitudes determined a 'zero-force' trajectory along which the prosthesis actuator torque was zero. Displacement from that trajectory evoked torque determined by mechanical impedance that was implemented as position and velocity feedback to a highly-back-drivable electro-mechanical actuator. The sum of EMG amplitudes determined the prosthesis mechanical impedance, mimicking the action of natural muscles [1]. Comparison of this controller with conventional velocity control (difference of EMG amplitudes determined prosthesis angular velocity with high mechanical impedance) showed a marked superiority, especially in tasks requiring coordination of natural and artificial joints (e.g. accommodation of a kinematic constraint as in turning a crank), bi-manual coordination and production of mechanical work [3, 86].

7 Combining Motion and Interaction Primitives

An important question is how interactive and motion primitives work together to enable and potentially simplify dexterous manipulation. Two distinct domains are involved. Motion planning belongs in the domain of 'signals' or information-processing, which permeates conventional computation and control theory.

Information-processing operations are *uni-directional* (input affects output but not vice-versa) and the only constraints appear to be temporal causality (no output before input) and boundedness (no infinite quantities). In contrast, interactions due to physical contact are fundamentally *bi-directional*—each system affects the other with mutual causality, as expressed in Newton's 3rd law [79]. They are subject to the numerous additional constraints that arise from the storage and transmission of energy, e.g. conservation of energy, production of entropy, etc.

A combination of dynamic behavior arising from computational information-processing with that arising from physical systems may be described in a unified framework by re-purposing and extending a remarkably effective tool of engineering analysis, the *equivalent electric circuit*. A comprehensive history of this concept is presented by Johnson [54, 55]. Originally Helmholtz and later (independently) Thévenin showed that any electric circuit containing electromotive forces (voltage sources) and resistors could be replaced at any pair of terminals by a single voltage source in series with a single resistor [34, 105]. Subsequently Mayer and Norton simultaneously (and independently) formulated an equivalent electric circuit composed of a current source in parallel with a resistor [75, 81]. The concept of impedance introduced by Heaviside and its dual, admittance, allowed equivalent electric circuits to be extended to include dynamic behavior (e.g. capacitance and inductance) [32, 33].

An electric circuit comprising *arbitrarily complicated* networks of voltage sources, current sources, and linear resistors, capacitors and inductors may be represented by a Thévenin or Norton equivalent circuit. At a terminal pair where the circuit interacts with its environment—an *interaction port*—it behaves as though composed of only two parts with a simple connection. Moreover, each of those parts may be identified unambiguously by simple experiments performed at the interaction port. This prodigious simplification is one reason why equivalent circuits remain a core conceptual tool of engineering analysis.

An equivalent circuit describes an interface between the domain of signals and the domain of energy. In an audio amplifier, signals with negligible power (e.g. retrieved from a storage medium or synthesized by a computer) control some of the amplifier's internal voltage and/or current sources which act to deliver substantial power to a loudspeaker, thereby generating sound energy. An equivalent circuit 'parses' the dynamics of the entire audio amplifier into two pieces. The Thévenin or Norton equivalent source describes the 'forward-path' dynamics relating the low-power input signals to the high-power electrical excitation delivered to the loudspeaker—independent of interaction with the loudspeaker. The equivalent admittance or impedance describes the dynamics of the high-power interaction between the amplifier and the loudspeaker—independent of the forward-path dynamics.

The equivalent circuit concept may be re-purposed to describe the relation between the dynamics of computational information processing and the dynamics of physical systems. The 'equivalent source' (Thévenin or Norton) describes unidirectional forward path dynamics through which computation may influence physical events. The 'equivalent resistance' (admittance or impedance) describes bidirectional dynamic interactions through which physical events evoke a physical response.

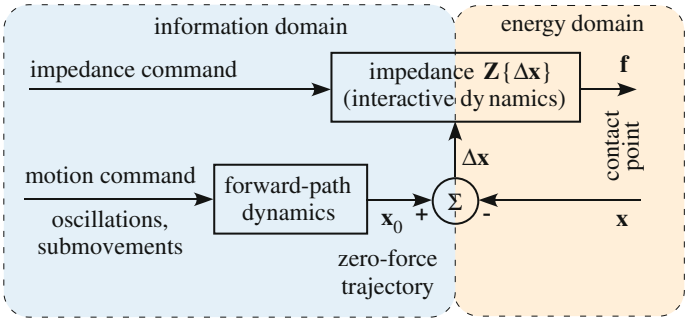

Fig. 7 A nonlinear equivalent network relating the information and energy domains of dynamic behavior. Reproduced from [43]

Equivalent circuits were originally applied to electrical systems with linear dynamics. The concept is readily extended to non-electrical systems though, as general physical systems do not necessarily form closed circuits, the term 'equivalent network' is more appropriate. The concept may further be extended to important classes of nonlinear systems, especially actuators (including mammalian muscles) which occupy the interface between physical and informational dynamics [43].

Extending classical circuit theory to nonlinear systems combining informational and physical dynamics provides a *unified* description of how central commands and peripheral mechanics cooperate to produce observable behavior (Fig. 7). It specifies how three classes of dynamic primitives may be related. Independent of interaction with the environment, the 'equivalent source' describes the nominal unidirectional forward-path dynamic response to central commands, which may consist of submovements and oscillations. Bidirectional interactive dynamics (also modifiable by central commands) are characterized by mechanical impedances. These two parts, *unidirectional* and *bidirectional*, can be identified unambiguously by simple experiments [43]. This disambiguation teases apart the contributions of mechanical dynamics and the problems solved by computation.

8 Identifying the Equivalent Source Without 'Opening the Box'

The challenge of describing and detailing human interactive dynamics is particularly acute. First, the biological actuator (muscle) has notoriously complicated and highly nonlinear dynamics [112]. Second, the neural control system is prodigiously complicated and largely uncharted [56]. Third, there is as yet no ethical way to 'open the box' and reliably observe relevant variables internal to the human neural control system. To date, imaging technologies provide only a coarse-grained measure of limited parts of this system. If applicable, an equivalent network representation could

summarize all of that complexity in a few elements that could (at least in principle) be identified unambiguously from external measurements.

Can the equivalent source be identified during movement, i.e. when commands from the central nervous system are changing? Several attempts have been made by assuming a reasonable form for interactive dynamics (e.g. time-varying mass-spring-and-damper behavior), identifying parameters of that model, and extrapolating from the results. Unfortunately, the outcome is exquisitely sensitive to the assumed form of the model—see [30] but compare with [31]. In fact, even the *order* of interactive dynamics is not reliably known. For example, though it is reasonable to assume that high-frequency behavior is dominated by skeletal inertia, yielding 2nd order dynamics, in fact there is evidence of anti-resonance due to muscle mass moving relative to skeletal inertia, and that requires higher-order dynamics [108, 109].

However, an equivalent network motion source can, in principle, be identified without *any* knowledge of the neuro-muscular actuator impedance. A workable method to do so during arm movements was presented in [36]. The essence of the method was to estimate multi-variable skeletal inertia, then generate exogenous forces with a robotic manipulandum so that the neuro-muscular forces were nominally zero throughout a discrete reaching movement. The resulting trajectory was the motion source of an equivalent network model of the neuro-muscular actuator. Iteration over several nominally-identical movements was required to improve the estimate and the exogenous forces were presented only on randomly selected movements to preclude human adaptation to the stimulus. Passing over the details, which are presented in [35, 36], a significant result was that, despite the intrinsic variability of human motor control, the method converged rapidly. The result was a reliable estimate of the motion source output, independent of any assumptions about neuro-muscular mechanical impedance.

9 The Preferred Form of Equivalent Network Models

A linear equivalent circuit may be expressed in four different and fully interchangeable ways: there are two choices for the equivalent source (Thévenin or Norton) and two choices for the operational form of the interactive dynamics (admittance or impedance—force in, motion out or *vice versa*). A nonlinear equivalent network is more restricted. Because a nonlinear dynamic operator may not have a well-defined inverse, the interactive dynamics may be expressible in only one of the two operational forms (admittance or impedance). For example, mammalian muscle is always well-defined in impedance operational form (motion in, force out) but not necessarily in admittance operational form.

The type of source may also be restricted. Key properties of physical system dynamics manifest as symmetries or invariances—features that do not change when other factors do. Noether's theorem famously identifies conservation principles with symmetries (e.g. energy conservation with time-shift invariance, etc.) [106]. One desirable geometric symmetry for interactive dynamics is *translation invariance*. If

the reference frame origin is translated, interactive behavior should not change. That is, the commands required to perform a contact task should ideally be identical at all locations. While this may be challenging in some cases—a fixed-based robot's limited workspace obviously limits translation invariance to within its reach—it is highly desirable, at least within a region near the center of the robot's workspace. Translation invariance restricts the choice of equivalent source as follows.

For many contact and interaction tasks it seems natural for the forward path dynamics to specify a nominal force (or torque) $\mathbf{f}_0(t)$. Examples include the nominal force that must be exerted by the feet on the ground during normal locomotion; averaged over a gait cycle, the net vertical foot-ground force must equal the vehicle's (or animal's) weight. Interactive dynamics (in impedance operational form) $\mathbf{Z}\{\cdot\}$ modify that nominal force based on actual motion $\mathbf{x}(t)$, $\mathbf{f}(t) = \mathbf{f}_0(t) - \mathbf{Z}\{\mathbf{x}(t)\}$.

To clarify the following argument, consider that impedance is like a dynamic, nonlinear version of a linear spring of stiffness k. In one dimension $f = f_0 - kx$. Further consider translating the coordinate frame to a new origin so that $x^{'} = x + c$ where c is a constant. In the new coordinate frame $f^{'} = (f_0 + kc) - kx'$. In this case, the translated 'force source' is $f_0^{'} = f_0 + kc$. This is *not* translation invariant; it depends both on the origin of the coordinate frame c and on the stiffness k. The latter is especially troubling as it compromises the separation of forward path dynamics from interactive dynamics—yet that is one of the particular advantages of an equivalent network representation.

Instead, consider an equivalent network with forward path dynamics that specifies a nominal or 'zero-force' motion $\mathbf{x}_0(t)$. Interactive dynamics (in impedance operational form) generate forces in response to deviations of actual motion from nominal motion $\mathbf{f}(t) = \mathbf{Z}\{\Delta\mathbf{x}(t)\}$ where $\Delta\mathbf{x}(t) = \mathbf{x}_0(t) - \mathbf{x}(t)$. As above, impedance is like a dynamic, nonlinear version of a linear spring of stiffness k. In one dimension $f = k(x_0 - x)$. Again consider translating the coordinate frame to a new origin so that $x^{'} = x + c$. With $x_0^{'} = x_0 + c$, $\Delta x^{'} = \Delta x$, hence $f^{'} = f$ and $k^{'} = k$ or, more generally, $\mathbf{Z}^{'}\{\cdot) = \mathbf{Z}\{\cdot\}$. The advantages of an equivalent network representation have been preserved.

Maxwell identified a correspondence between electrical and mechanical systems, with electrical voltage analogous to mechanical force and current to velocity [74]. Using that analogy, a Norton equivalent network (i.e. with a motion source) is translation invariant whereas a Thévenin equivalent network (i.e. with a force source) is not. Both the structure of the mathematical representation and (more important) the separation of forward path dynamics from interactive dynamics are independent of the choice of coordinate frame origin. It is interesting (and probably no coincidence) that a Norton equivalent network also permits unambiguous identification of the source term from observations made at the interaction port, while a Thévenin equivalent network does not [43].

Summarizing, actuators such as muscles are at the interface between the computational dynamics of the information domain and the physical dynamics of the energy domain. A nonlinear equivalent network provides a competent 'canonical model' of these dynamic objects that may be used to compare alternatives. An equivalent network of the Norton (motion source) type appears to be superior, both unambigu-

ously identifiable and invariant under coordinate frame translation. This may seem counter-intuitive as some tasks seem naturally to require specification of nominal forces. Nevertheless, the more robust description is in terms of nominal motion.

Remarkably, the human motor control system exhibits a strong preference to plan motions rather than forces. Point-to-point reaching movements are generally executed by an approximately straight, smooth hand path [29]. Exposed to mechanical perturbations, subjects spontaneously adapt their muscle forces to restore an approximately straight, smooth hand path [64, 95]. Exposed to a distorted mapping between motion of the hand and motion of a cursor on a screen, subjects spontaneously adapt their hand path to restore an approximately straight, smooth path of the screen cursor [28]. This emphasis on motions is the basis of a successful robot-aided approach to neuro-recovery [46].

10 Choosing Task-Specific Impedance

The most appropriate physical interaction dynamics varies with the task to be accomplished. One effective way to choose that dynamic behavior is to describe the task as an optimization problem. Optimization is a powerful and general approach to robot motion planning which has become more practical with advances in both computational speed and algorithmic sophistication [21, 62].

For optimization to yield specifications for interactive dynamics, the objective function to be optimized should include terms involving both motion and 'exertion' at the interaction port. The term motion is here intended as an 'umbrella' label for velocity and its integrals and derivatives (e.g. displacement, acceleration, etc.) The term exertion is here intended as an 'umbrella' label for force and its integrals and derivatives (momentum, force rate, etc.) The essential distinction between motion and exertion is articulated in [43]. An interaction port is defined by any set of motion variables and their energetic conjugates such that energy and its integrals or derivatives are well-defined. Thus mechanical work is defined by $W = \int \mathbf{f}^T d\mathbf{x}$ where $\mathbf{f}$ is a vector of forces or torques and $d\mathbf{x}$ is a vector of translational or angular displacements. The displacements need not refer to the same physical location (e.g. they may be displacements of a robot's several degrees of freedom) provided the corresponding forces are energetic conjugates such that work is correctly defined.

A simple 'toy' example may illustrate the point. Assume a manipulator and its control system are modeled as a mass m_m moving in 1 degree of freedom, retarded by linear damping b and driven by a linear spring referenced to a 'zero-force' point x_0. With no interaction force, $m_m\ddot{x} + b\dot{x} = k(x_0 - x)$. Assume the manipulator interacts with an object modeled as mass m_o such that both move with common motion x. The connection between manipulator and object is an interaction port, and the force exerted by the manipulator on the object is $f_o = m_o\ddot{x}$. Further assume the object is subject to stochastic perturbation forces w_e, modeled as zero-mean Gaussian white noise of strength S. Defining $m = m_m + m_o$, state-determined equations for the coupled system are

$$\frac{d}{dt}\begin{bmatrix} x \\ v \end{bmatrix} = \begin{bmatrix} 0 & 1 \\ -k/m & -b/m \end{bmatrix}\begin{bmatrix} x \\ v \end{bmatrix} + \begin{bmatrix} 0 \\ k/m \end{bmatrix} x_0 + \begin{bmatrix} 0 \\ 1/m \end{bmatrix} w_e$$

$$f_o = \left[-\frac{m_o}{m}k - \frac{m_o}{m}b\right]\begin{bmatrix} x \\ v \end{bmatrix} + \left[\frac{m_o}{m}k\right] x_0$$

The objective function should include force and displacement at the interaction port. Define displacement $\Delta x = x_0 - x$ and the objective function

$$Q = E\left\{\frac{1}{t_{final}}\int_0^{t_{final}} \left(\frac{f_o^2}{f_{tol}^2} + \frac{\Delta x^2}{\Delta x_{tol}^2}\right) dt\right\}$$

where f_{tol} and Δx_{tol} are tolerances on interface force and displacement. The state (x, v) and output f_o are random variables due to the presence of the stochastic input. The expectation operator $E\{\cdot\}$ makes the objective Q a deterministic scalar. The stochastic perturbation is included only to ensure the optimization yields non-trivial stable solutions. Once a solution with non-zero noise strength S has been identified, we may consider the limit as the noise strength approaches zero.

For simplicity, assume $x_0(t) = \text{constant} = 0$; i.e. the object is to be held at a constant position despite perturbations. A summary of subsequent analysis is presented in an appendix, based on a method presented in [38, 41]. A steady-state solution for the optimal stiffness and damping is

$$\lim_{S\to 0} k_{opt} = \frac{m_m + m_o}{m_o}\frac{f_{tol}}{\Delta x_{tol}}$$

$$\lim_{S\to 0} b_{opt} = \sqrt{2k_{opt}(m_m + m_o)}$$

The optimal damping coefficient b_{opt} is such that the 2nd order coupled system (manipulator plus object) has a dimensionless damping ratio of $\zeta = b_{opt}/2\sqrt{k_{opt}(m_m + m_o)} = \sqrt{2}/2$. As a result the 2nd order frequency response function relating object motion to perturbations is 'optimally flat' up to a break frequency defined by the optimal stiffness and the total mass, manipulator plus object.

The optimal stiffness k_{opt} is proportional to the ratio of force tolerance to displacement tolerance. That is physically reasonable; if an object is delicate and cannot tolerate large applied forces, the manipulator should be compliant in proportion. Perhaps less obvious is that the optimal stiffness is also proportional to the ratio $(m_m + m_o)/m_o$ of total mass (manipulator plus object) to object mass. As a result the 2nd order frequency response function relating object motion to perturbations has a break frequency Ω_{break} independent of manipulator mass.

$$\Omega_{break} = \sqrt{\frac{k_{opt}}{m_m + m_o}} = \sqrt{\frac{1}{m_o}\frac{f_{tol}}{\Delta x_{tol}}}$$

A minimal stiffness $k_{opt} = f_{tol}/\Delta x_{tol}$ of would be obtained if the object mass was much larger than the manipulator mass apparent at the interaction port. That may be achieved with some of the newer designs of back-drivable or compliant robot 'hands' or end-effectors [83]. Unfortunately, the converse is usually true. For a typical robot, the mass apparent at its gripper dwarfs the mass of the objects it can manipulate. Greater manipulator apparent mass implies greater optimal stiffness for the same ratio of force and displacement tolerances.

Despite its simplicity, this 'toy' example may provide insight. Apparent mass matters, even if the emphasis is on choosing the optimal stiffness, e.g. to be implemented via one of the recent variable-stiffness actuator designs [11, 107]. Apparent mass includes actuator inertia, 'reflected' or transformed through the transmission system relating end-effector motion to actuator motion. Electro-mechanical robot transmissions commonly include high-ratio gear trains to amplify motor torques. That dramatically increases the motor's contribution to end-effector apparent mass, which is proportional to the square of the gear ratio. A recent study of a commercially-available robot showed that the contribution of its motors to end-effector apparent mass was more than 2.5 times the contribution of its link segments [49].

This 'toy' example also hints at one of the challenges of choosing impedance. Constructing an objective function to include terms involving both motion and 'exertion' at an interaction port is straightforward but solving the resulting optimization problem is not. Even this linear 1 degree of freedom example with 2nd order dynamics required solving 6 simultaneous nonlinear differential equations, and only a steady-state solution was presented (see Appendix). The complexity of the computational problem may be expected to grow exponentially with the number of degrees of freedom and the order of the dynamics associated with each degrees of freedom. Some tasks—especially if they require active vibration absorption—will require higher-order interaction dynamics. Furthermore, a general task will require a time-varying 'trajectory' of impedances rather than a steady-state time-invariant solution. Powerful methods for numerical optimization are now available but unfortunately, variable impedance makes the optimization non-convex, and this appears to be fundamental. Nevertheless, despite the formidable challenges, solutions have been presented [12, 13, 72]. Advances in computational algorithms and processing power may be expected to yield further progress.

11 Using Composability to Meet Multiple Task Objectives

Unlike the 'toy' example above, realistic tasks may have multiple objectives which may present conflicting requirements. In addition, realistic tasks are commonly performed against the backdrop of other ongoing activities, which may interfere. For

example, fly-casting is usually performed from a standing position. The required arm motions generate inertial and gravitational perturbations to balance and posture; in turn, changing posture influences those arm motions. In principle, multiple conflicting goals may be incorporated into a single optimization problem; indeed, a well-formulated objective function must quantify some compromise between conflicting requirements if a non-trivial solution is to be identified. In principle, all of the human body's roughly 200 degrees of freedom could be included in the dynamics of the system to be optimized. Unfortunately, the exponential growth of computational complexity with degrees of freedom renders all but the simplest problems infeasible; this is Richard Bellman's notorious 'curse of dimensionality'.

Even if continuing advances in algorithms and processor speed may push back the boundaries of what can be computed in practice, it seems doubtful that global optimization is the best description of processes underlying human motor control. The *composability* of dynamic primitives provides an alternative. 'Composability' refers to the fact that dynamic primitives may be combined to produce more complex behavior. Experimental evidence indicates that some human movements are composed of a sequence of overlapping submovements (Figs. 4, 5 and 6). Oscillatory movements may also be combined, though there appears to be a strong preference for a limited set of phase relations between component oscillations [58, 59, 98, 99, 104]. Mechanical impedances are also composable. Remarkably, multiple impedances may be combined by *linear* superposition, even if the interactive dynamic relations they embody are *nonlinear* [39, 41]. This is due to a fact of Newtonian mechanics: an inertial object such as the skeleton or a tool determines acceleration in response to the linear sum of forces to which it is subjected.

Taking advantage of composability can dramatically simplify control. A simple example illustrates this point. Exerting force on a tool requires producing a concomitant minimum stiffness [90]. Expressed as an equivalent network, the required static behavior may be written as $f = k\,(x_0 - x)$ where f, k and x are end-point force, stiffness and position and x_0 is the zero-force position. This may be transformed to joint coordinates as $\tau = J^T\,(\theta)\,k\,(x_0 - L\,(\theta))$ where τ and θ are joint torque and angle, $x = L\,(\theta)$ describes the forward kinematics and $J\,(\theta)$ its derivative, the Jacobian matrix. With a high-level controller that specifies k and x_0 and controllable-torque actuators, that expression may be implemented as a nonlinear joint-space controller to achieve the specified end-point equivalent network behavior.

With kinematic redundancy—more joint than end-point degrees of freedom ($\dim\theta > \dim x$)—that equivalent network alone is insufficient to control configuration. Many joint configurations θ yield the same stiffness $f = k\,(x_0 - x)$ and 'null-space' motions that leave x unchanged are unaffected by this controller. However, configuration may be managed by a controller that implements a joint-space equivalent network behavior $\tau_j = K\,\Delta\theta = K\,(\theta_r - \theta)$ where K is a non-singular joint-space stiffness and θ_r is a zero-torque configuration. Even though one of these controllers is nonlinear, they may be superimposed by simple addition to achieve desirable behavior, $\tau_{net} = \tau + \tau_j = J^T\,(\theta)\,k\,(x_0 - L\,(\theta)) + K\,(\theta_r - \theta)$. This composite controller readily manages redundant degrees of freedom. Importantly, *inversion of the kinematic equations is not required*. Not only is a difficult computational

problem avoided but, unlike controllers that fundamentally require inversion of the kinematic equations, this approach is indifferent to kinematic singularities. It can operate *at and into* kinematic singularities (e.g. at maximum reach).

12 Modulating Inertia via Multi-limb Coordination

Managing redundant degrees of freedom is especially important for modulating inertial behavior, which dominates interactive dynamics at the transitions between free and constrained motion. Modulating a robot's inertial behavior using feedback control is challenging. It usually requires expensive and delicate force/torque sensors. Moreover, the extent of feedback modulation of inertial behavior is severely constrained if contact stability is to be guaranteed [14, 16]. However, choosing the configuration of the joints has a profound influence on the inertial behavior apparent at a point of contact such as the hand [40]. Importantly, it allows inertial dynamics, which determine the magnitude of impulsive forces, to be *pre-tuned prior to contact* thereby avoiding possible problems with time delays due to reactive control.

The advantages of dynamic primitives and the composability of impedance extend to multi-limb coordination. Controlling inertia with a single limb is challenging due to the distribution of physical inertia along the limb segments. In particular, translational force impulses almost always induce undesirable rotational motion. In contrast, two-handed control of interaction with a tool affords advantages. In particular, with two hands, the inertial terms that couple translational impulses to rotational motion can be made to cancel, making the response to the collision that occurs on contact fundamentally more predictable.

Unfortunately, wielding a tool with two hands 'closes the kinematic chain' relating joint motions to end-point motions. Closed-chain kinematic equations are notoriously challenging. However, *this challenge may be avoided entirely* by taking advantage of the composability of impedance. If the motion of the two hands at the point of contact with the tool is common (more generally, if they are kinematically related through the tool) their interactive behaviors superimpose linearly. Each limb may be endowed with stiffness as described above based on the *open-chain* kinematics of each limb separately (and without inverting its kinematic equations). The net stiffness of both arms interacting with the tool is simply the sum of their individual stiffnesses. The net inertia of both arms interacting with the tool is the sum of their individual inertias. The undesirable coupling terms of the 'left' arm are generally equal and opposite to those of the 'right' arm; combined, they cancel.

The above considered only stiffness and inertia. Dissipative behavior (e.g. damping) is also important, indeed essential to ensure stability. Once again, the composability of impedance allows damping terms to be implemented independent of stiffness or inertia, separately for each limb (or even for each joint), then combined by simple superposition. Higher-order dynamic terms, should they be relevant, may be treated in an exactly analogous manner. Moreover, if each of these terms, singly or in combination, is configured to exhibit attractor dynamics, then it becomes a

dynamic primitive in the sense that we have defined [47, 48]. This, in turn, confers an important robustness to the behavior implemented.

13 Advantages and Consequences of Composability

The composability of dynamic primitives provides one way to 'work around' the curse of dimensionality, allowing the challenge of coordinating many degrees of freedom in a multi-objective task to be broken down into a set of much smaller problems. Each sub-task may be expressed in the form of an equivalent network (Fig. 7) which combines uni-lateral forward-path dynamic behavior, which outputs a zero-force trajectory $x_0(t)$, with bi-lateral interactive dynamic behavior, the impedance $Z\{\cdot\}$. Each equivalent network responds to the motion of the inertial object with which it interacts. Interactions may be at different locations; for example, one equivalent network may specify a desired behavior of the hand, another a desired behavior of the elbow, and so forth. In this way, different body parts may be used to 'manipulate' the world, even simultaneously; humans do this frequently. Each equivalent network determines an output force or torque which adds to the net force or torque applied to the inertial object (e.g. the skeleton) and produces force or motion, depending on the totality of all interacting equivalent networks and physical objects (e.g. tools). If conflicting goals are expressed by different equivalent networks, their respective impedances determine the resolution. Coordination emerges from the combined action of all equivalent networks. Because of its generality, this approach has been extended to non-contact tasks such as avoiding obstacles while acquiring targets, even obstacles which may move [6, 41, 78].

This '*divide et impera*' approach may have interesting consequences. Using it as outlined above to manage kinematic redundancy, to ensure control of configuration the joint-space stiffness matrix K must be positive-definite. Its inverse exists, defining a joint-space compliance $\Delta\theta = K^{-1}\tau_j$. For small $\Delta\theta$, the corresponding end-point compliance is $\Delta x \cong J(\theta) K^{-1} J^T(\theta) f$, where $\Delta x = x - x_r = x - L(\theta_r)$.[3] The end-point compliance $c_j(\theta) = J(\theta) K^{-1} J^T(\theta)$ provides a 'default' interactive behavior which renders force control difficult. Its inverse[4] determines a minimum end-point stiffness. Even with extremely back-drivable actuators (e.g. current-controlled electric motors) 'perfect' force control, corresponding to infinite compliance or zero stiffness, cannot be achieved. Of course, this is also a limitation of human motor control. Whether this is a disadvantage (a 'bug') or an advantage (a 'feature') depends on context. As outlined above, in most tool-using tasks, simultaneous modulation of stiffness and force is essential.

[3] This result may be extended to large $\Delta\theta$ and Δx: for any Δx imposed within the workspace, at equilibrium the linkage assumes a pose that minimizes total potential energy; the analysis is omitted for brevity.

[4] When it can be computed; in some configurations and some directions, e.g., arm fully outstretched, compliance approaches zero and stiffness approaches infinity.

14 Integrating Tool Use with Posture, Balance and Locomotion

The composability of dynamic primitives may simplify the control of complex behavior, and using mechanical impedance to manage physical interaction may facilitate integration of arm motion with posture, balance and locomotion. Indeed, consideration of posture is essential to understand contact tasks and force control. Many tools are used from a standing position. In that case the dynamics of force production depends critically on the posture of the feet. Pushing hard by leaning with the feet together introduces an unstable dynamic zero—force must transiently increase before it can decrease and vice versa. Spreading the feet apart eliminates this behavior—foot pose affects hand dynamics [88].

However, the precise nature of dynamic motion primitives underlying posture and locomotion is unclear. At first blush it might seem that a point attractor is the appropriate dynamic primitive for posture and balance, but time-series analysis of center of pressure variation during standing indicates that multiple limit cycles are present [17, 25]. Rhythmic walking might seem to require a limit-cycle attractor and, consistent with this model, human walking exhibits entrainment to periodic perturbations, both on a treadmill and overground [4, 5, 82]. However, rhythmic walking might alternatively emerge as a consequence of a 'capture point' foot-placement strategy: the swing foot is placed at a location where present momentum would bring the body to rest over it; observations of human walking appear consistent with this model [24, 87, 110].

Unimpaired human walking is highly dynamic, to the extent that it may be regarded as 'controlled falling'; during single-leg stance the system is unstable (like an inverted pendulum). From that perspective, one important function of the foot—and especially the ankle—is analogous to the function of an automobile shock-absorber, acting to 'catch' the descending body. The essential 'shock-absorbing' behavior is characterized by mechanical impedance. While neural feedback of motion and force contributes to net mechanical impedance, the delays due to neural transmission render feedback modulation of mechanical impedance ineffective during the rapid events associated with heel-strike. Consequently, we may expect ankle/foot mechanical impedance to be pre-tuned prior to heel-strike. Observations of multi-variable human ankle mechanical impedance show that it is reliably increased by simultaneous co-activation of opposing muscles [65, 66, 69, 71]. Furthermore, observations of the time-varying 'trajectory' of ankle mechanical impedance during treadmill walking show that it is elevated by co-contracting opposing muscles prior to heel-strike [67, 70]. Remarkably, these measurements also show that ankle mechanical impedance is *energetically passive*, even when muscles are active (up to 30% of maximum voluntary contraction) [68]. The significance of this observation is that, in general, physical interaction (e.g. due to foot-ground contact) might compromise stability. Energetic passivity guarantees that physical contact cannot induce instability [15].

Summarizing, while it is clear that dynamic primitives such as oscillations and mechanical impedances likely play an important role in posture and locomotion, many of the details of how this is accomplished remain to be uncovered.

15 A Geometry of Dynamic Primitives?

The paradox of human performance—how do we out-perform modern robots despite inferior 'wetware' and 'hardware'?—is both a challenge and opportunity. The challenge is to understand how it is done; the opportunity is to identify bio-inspired approaches to improve robot performance. This may require substantial re-thinking of robot control, even down to the fundamentals of the underlying geometry. Model-based robot control implicitly assumes a Riemannian geometry, yet human haptic perception appears to be incompatible with Riemannian geometry.

A growing body of evidence suggests that human motor performance is based on dynamic primitives. Combinations of motion primitives (submovements and oscillations) account for recovery after neurological injury as well as some counter-intuitive limitations of human motor control (moving slowly is hard for humans). Controlling physical interaction may also be based on interactive dynamic primitives (impedance or admittance). Forward-path dynamics and interactive dynamics may be combined by re-purposing and extending the classical linear equivalent electric circuit to define a nonlinear equivalent network.

Interestingly, the most useful form of nonlinear equivalent network requires the forward-path dynamics to prescribe motions, not forces. That is consistent with unimpaired human motor behavior and recovery after neural injury. It suggests some form of underlying geometric structure but prompts an open question: Which geometry is induced by a composition of motion and interactive dynamic primitives? What are its properties? Answering those questions might pave the way to achieve superior robot control and seamless human-robot collaboration.

Acknowledgements I would especially like to acknowledge Professor Dagmar Sternad's seminal contribution to the concepts of dynamic primitives presented herein. This work was supported in part by the Eric P. and Evelyn E. Newman Fund and by NIH Grant R01-HD087089 and NSF EAGER Grant 1548514.

Appendix: Choosing Impedance via Stochastic Optimization

Assume a manipulator and its control system are modeled as a mass m_m moving in 1 degree of freedom, retarded by linear damping b and driven by a linear spring referenced to a 'zero-force' point x_0. It interacts with an object modeled as mass m_o such that both move with common motion x. State-determined equations for the coupled system are

$$\frac{d}{dt}\begin{bmatrix} x \\ v \end{bmatrix} = \begin{bmatrix} 0 & 1 \\ -k/m & -b/m \end{bmatrix}\begin{bmatrix} x \\ v \end{bmatrix} + \begin{bmatrix} 0 \\ k/m \end{bmatrix} x_0 + \begin{bmatrix} 0 \\ 1/m \end{bmatrix} w_e$$

$$f_o = \left[-\frac{m_o}{m}k - \frac{m_o}{m}b\right]\begin{bmatrix} x \\ v \end{bmatrix} + \left[\frac{m_o}{m}k\right] x_0$$

where $m = m_m + m_o$, f_o is the force exerted by the manipulator on the object, and w_e denotes stochastic perturbation forces, modeled as zero-mean Gaussian white noise of strength S, i.e. $E\{w_e(t)\} = 0$, $E\{w_e(t)\, w_e(t+\tau)\} = S\delta(\tau)$, where $E\{\cdot\}$ is the expectation operator and $\delta(\cdot)$ denotes the unit impulse function. The objective function to be minimized is

$$Q = E\left\{\frac{1}{t_{final}}\int_0^{t_{final}} \left(\frac{f_o^2}{f_{tol}^2} + \frac{\Delta x^2}{\Delta x_{tol}^2}\right) dt\right\}$$

where $\Delta x = x_0 - x$ and f_{tol} and Δx_{tol} are tolerances on interface force and displacement. Due to the stochastic input, the state $(x(t), v(t))$ and output $f_o(t)$ are random variables. Assume $x_0(t) = \text{constant} = 0$ and find conditions for a steady-state solution (i.e. consider the limit as $t_{final} \to \infty$). The mean state and output variables propagate deterministically, i.e. $E\{x(t)\} = E\{v(t)\} = E\{f_o(t)\} = 0$. Define the input covariance $W_e(t) = E\left\{\left(w_e^2(t)\right)\right\} = S$ and the state covariance matrix

$$\Sigma(t) = E\left\{\begin{bmatrix} x(t) \\ v(t) \end{bmatrix}\begin{bmatrix} x(t) & v(t) \end{bmatrix}\right\} = E\left\{\begin{bmatrix} x^2(t) & x(t)\, v(t) \\ x(t)\, v(t) & v^2(t) \end{bmatrix}\right\}$$

For notational convenience, omit the explicit time dependence and use overbar notation $\Sigma = \begin{bmatrix} \overline{x^2} & \overline{xv} \\ \overline{xv} & \overline{v^2} \end{bmatrix}$. Covariance propagation through a linear time-invariant system is described by the dynamic equation $\dot{\Sigma} = A\Sigma + \Sigma A^T + BSB^T$ where A and B are system and input weighting matrices.

$$\frac{d}{dt}\begin{bmatrix} \overline{x^2} & \overline{xv} \\ \overline{xv} & \overline{v^2} \end{bmatrix} = \begin{bmatrix} 2\overline{xv} & \overline{v^2} - \overline{x^2}k/m - \overline{xv}b/m \\ \overline{v^2} - \overline{x^2}k/m - \overline{xv}b/m & -2\overline{xv}k/m - 2\overline{v^2}b/m \end{bmatrix} + \begin{bmatrix} 0 & 0 \\ 0 & 1/m^2 \end{bmatrix} S$$

Re-write as 3 coupled scalar differential equations

$$\begin{aligned} \tfrac{d}{dt}\overline{x^2} &= 2\overline{xv} \\ \tfrac{d}{dt}\overline{xv} &= \overline{v^2} - \overline{x^2}k/m - \overline{xv}b/m \\ \tfrac{d}{dt}\overline{v^2} &= S/m^2 - 2\overline{xv}k/m - 2\overline{v^2}b/m \end{aligned}$$

The scalar to be minimized is

$$Q = \frac{1}{t_{final}} \int_0^{t_{final}} \left(\frac{\overline{f_o^2}}{f_{tol}^2} + \frac{\overline{\Delta x^2}}{\Delta x_{tol}^2} \right) dt$$

$$f_o^2 = \left(\frac{m_o^2}{m^2} \right) \left(k^2 x^2 + 2kbxv + b^2 v^2 \right)$$

Defining $q = (f_{tol}/\Delta x_{tol})(m/m_o)$

$$Q = \frac{1}{f_{tol}^2} \frac{m_o^2}{m^2} \frac{1}{t_{final}} \int_0^{t_{final}} \left(k^2 \overline{x^2} + 2kb\overline{xv} + b^2 \overline{v^2} + q^2 \overline{x^2} \right) dt$$

Construct the 'control Hamiltonian'

$$\begin{aligned} H = &\left(k^2 + q^2\right) \overline{x^2} + 2kb\overline{xv} + b^2 \overline{v^2} \\ &+\lambda_1 2\overline{xv} \\ &+\lambda_2 \left(\overline{v^2} - \overline{x^2} k/m - \overline{xv} b/m \right) \\ &+\lambda_3 \left(S/m^2 - 2\overline{xv} k/m - 2\overline{v^2} b/m \right) \end{aligned}$$

where λ_i denote Lagrange multipliers. Minimize with respect to k and b.

$$\begin{aligned} \frac{\partial H}{\partial k} &= 2k\overline{x^2} + 2b\overline{xv} - \lambda_2 \overline{x^2}/m - \lambda_3 2\overline{xv}/m = 0 \\ \frac{\partial H}{\partial b} &= 2k\overline{xv} + 2b\overline{v^2} - \lambda_2 \overline{xv}/m - \lambda_3 2\overline{v^2}/m = 0 \end{aligned}$$

The Lagrange multipliers are defined by 'co-state' equations.

$$\begin{aligned} \frac{\partial H}{\partial \overline{x^2}} &= -\dot{\lambda}_1 = k^2 + q^2 - \lambda_2 k/m \\ \frac{\partial H}{\partial \overline{xv}} &= -\dot{\lambda}_2 = 2kb + 2\lambda_1 - \lambda_2 b/m - \lambda_3 2k/m \\ \frac{\partial H}{\partial \overline{v^2}} &= -\dot{\lambda}_3 = b^2 + \lambda_2 - \lambda_3 2b/m \end{aligned}$$

Assume steady state exists and set all rates of change to zero.

$$
\begin{gathered}
2\overline{xv} = 0 \\
\overline{v^2} - \overline{x^2}k/m - \overline{xv}b/m = 0 \\
S/m^2 - 2\overline{xv}k/m - 2\overline{v^2}b/m = 0 \\
k^2 + q^2 - \lambda_2 k/m = 0 \\
2kb + 2\lambda_1 - \lambda_2 b/m - \lambda_3 2k/m = 0 \\
b^2 + \lambda_2 - \lambda_3 2b/m = 0
\end{gathered}
$$

A little manipulation shows that

$$
\begin{gathered}
\overline{xv} = 0 \\
\overline{v^2} = \overline{x^2}k/m \\
\overline{x^2} = S/2kb \\
\overline{v^2} = S/2bm
\end{gathered}
$$

The first co-state equation yields

$$k^2 + q^2 = \lambda_2 k/m$$

$$\lambda_2 = km + q^2 m/k$$

The optimal stiffness is defined by

$$2k_{opt}\overline{x^2} = \lambda_2 \overline{x^2}/m$$

$$k_{opt} = q = \frac{f_{tol}}{\Delta x_{tol}} \frac{m}{m_o}$$

Note that this manipulation requires $\overline{x^2} \neq 0$ and hence $S \neq 0$. However, k_{opt} is independent of noise strength S.

The third co-state equation yields

$$b^2 + \lambda_2 = \lambda_3 2b/m$$

$$\lambda_3 = \left(b^2 + \lambda_2\right) m/2b = \frac{bm}{2} + \frac{km}{2b} + \frac{q^2 m^2}{2kb}$$

The optimal damping is defined by

$$2b_{opt}\overline{v^2} = \lambda_3 2\overline{v^2}/m$$

$$b_{opt} = \sqrt{2k_{opt}m}$$

This manipulation requires $\overline{v^2} \neq 0$ and hence $S \neq 0$. However, b_{opt} is independent of noise strength S.

References

1. C. Abul-Haj, N. Hogan, An emulator system for developing improved elbow-prosthesis designs. IEEE Trans. Biomed. Eng. **34**, 724–737 (1987)
2. C.J. Abul-Haj, N. Hogan, Functional assessment of control-systems for cybernetic elbow prostheses. 1. Description of the technique. IEEE Trans. Biomed. Eng. **37**, 1025–1036 (1990a)
3. C.J. Abul-Haj, N. Hogan, Functional assessment of control-systems for cybernetic elbow prostheses. 2. Application of the technique. IEEE Trans. Biomed. Eng. **37**, 1037–1047 (1990b)
4. J. Ahn, N. Hogan, A simple state-determined model reproduces entrainment and phase-locking of human walking dynamics. PLoS ONE **7**, e47963 (2012a)
5. J. Ahn, N. Hogan, Walking is not like reaching: evidence from periodic mechanical perturbations. PLoS ONE **7**, e31767 (2012b)
6. J.R. Andrews, N. Hogan, Impedance Control as a Framework for Implementing Obstacle Avoidance in a Manipulator, in BOOK, D. E. H. A. W. J. (ed.) *Control of Manufacturing Processes and Robotic Systems* (ASME, 1983)
7. A.J. Bastian, T.A. Martin, J.G. Keating, W.T. Thach, Cerebellar ataxia: abnormal control of interaction torques across multiple joints. J. Neurophysiol. **76**, 492–509 (1996)
8. A. Bissal, J. Magnusson, E. Salinas, G. Engdahl, A. Eriksson, On the design of ultra-fast electromechanical actuators: a comprehensive multi-physical simulation model, in *Sixth International Conference on Electromagnetic Field Problems and Applications (ICEF)* (2012)
9. T. Boaventura, C. Semini, J. Buchli, M. Frigerio, M. Focchi, D.G. Caldwell, Dynamic torque control of a hydraulic quadruped robot, in *IEEE International Conference on Robotics and Automation* (IEEE, Saint Paul, Minnesota, USA, 2012)
10. C. Boesch, H. Boesch, Tool use and tool making in wild chimpanzees. Folia Primatologica **54**, 86–99 (1990)
11. D.J. Braun, S. Apte, O. Adiyatov, A. Dahiya, N. Hogan, Compliant actuation for energy efficient impedance modulation, in *IEEE International Conference on Robotics and Automation* (2016)
12. J. Buchli, F. Stulp, E. Theodorou, S. Schaal, Learning variable impedance control. Int. J. Robot. Res. **30**, 820–833 (2011)
13. M. Cohen, T. Flash, Learning impedance parameters for robot control using an associative search network. IEEE Trans. Robot. Autom. **7**, 382–390 (1991)
14. E. Colgate, On the intrinsic limitations of force feedback compliance controllers, in *Robotics Research - 1989*, eds. by K. Youcef-Toumi, H. Kazerooni (ASME, 1989)
15. J.E. Colgate, N. Hogan, Robust control of dynamically interacting systems. Int. J. Control **48**, 65–88 (1988)
16. J.E. Colgate, N. Hogan, The interaction of robots with passive environments: application to force feedback control, in *Fourth International Conference on Advanced Robotics*, June 13–15 (Columbus, Ohio, 1989)
17. J.J. Collins, C.J. de Luca, Open-loop and closed-loop control of posture: a random-walk analysis of center-of-pressure trajectories. Exp. Brain Res. **95**, 308–318 (1993)
18. F. Crevecoeur, J. McIntyre, J.L. Thonnard, P. Lefèvre, Movement stability under uncertain internal models of dynamics. J. Neurophysiol. **104**, 1301–1313 (2010)
19. A. de Rugy, D. Sternad, Interaction between discrete and rhythmic movements: reaction time and phase of discrete movement initiation against oscillatory movements. Brain Res. **994**, 160–174 (2003)
20. S. Degallier, A. Ijspeert, Modeling discrete and rhythmic movements through motor primitives: a review. Biol. Cybern. **103**, 319–338 (2010)

21. R. Deits, R. Tedrake, Efficient mixed-integer planning for UAVs in cluttered environments, in *IEEE International Conference on Robotics and Automation (ICRA)* (IEEE, Seattle, WA, 2015)
22. J.A. Doeringer, N. Hogan, Intermittency in preplanned elbow movements persists in the absence of visual feedback. J. Neurophysiol. **80**, 1787–1799 (1998a)
23. J.A. Doeringer, N. Hogan, Serial processing in human movement production. Neural Netw. **11**, 1345–1356 (1998b)
24. J. Englsberger, C. Ott, A. Albu-Schaffer, Three-dimensional bipedal walking control based on divergent component of motion. IEEE Trans. Robot. **31**, 355–368 (2015)
25. C.W. Eurich, J.G. Milton, Noise-induced transitions in human postural sway. Phys. Rev. E **54**, 6681–6684 (1996)
26. E.D. Fasse, N. Hogan, B.A. Kay, F.A. Mussa-Ivaldi, Haptic interaction with virtual objects - spatial perception and motor control. Biol. Cybern. **82**, 69–83 (2000)
27. J. Flanagan, P. Vetter, R. Johansson, D. Wolpert, Prediction precedes control in motor learning. Curr. Biol. **13**, 146–150 (2003)
28. J.R. Flanagan, A.K. Rao, Trajectory adaptation to a nonlinear visuomotor transformation: evidence of motion planning in visually perceived space. J. Neurophysiol. **74**, 2174–2178 (1995)
29. T. Flash, N. Hogan, The coordination of arm movements - an experimentally confirmed mathematical model. J. Neurosci. **5**, 1688–1703 (1985)
30. H. Gomi, M. Kawato, Equilibrium-point control hypothesis examined by measured arm stiffness during multijoint movement. Science **272**, 117–120 (1996)
31. P. Gribble, D.J. Ostry, V. Sanguinetti, R. Laboissiere, Are complex control signals required for human arm movement? J. Neurophysiol. **79**, 1409–1424 (1998)
32. O. Heaviside, *Electrical Papers* (Massachusetts, Boston, 1925a)
33. O. Heaviside, *Electrical Papers* (Massachusetts, Boston, 1925b)
34. H.V. Helmholtz, II. Uber einige Gesetze der Vertheilung elektrischer Ströme in körperlichen Leitern mit Anwendung auf die thierisch-elektrischen Versuche [Some laws concerning the distribution of electrical currents in conductors with applications to experiments on animal electricity]. Annalen der Physik und Chemie **89**, 211–233 (1853)
35. A.J. Hodgson, Inferring Central Motor Plans from Attractor Trajectory Measurements, Ph.D, Institute of Technology, Massachusetts, 1994
36. A.J. Hodgson, N. Hogan, A model-independent definition of attractor behavior applicable to interactive tasks. IEEE Trans. Syst. Man Cybern. Part C- Appl. Rev. **30**, 105–118 (2000)
37. J.A. Hoffer, S. Andreassen, Regulation of soleus muscle stiffness in premammillary cats: intrinsic and reflex components. J. Neurophysiol. **45**, 267–285 (1981)
38. N. Hogan, Adaptive control of mechanical impedance by coactivation of antagonist muscles. IEEE Trans. Autom. Control **29**, 681–690 (1984)
39. N. Hogan, Impedance control - an approach to manipulation. 1. Theory. J. Dyn. Syst. Meas. Control Trans. Asme **107**, 1–7 (1985a)
40. N. Hogan, Impedance control - an approach to manipulation. 2. Implementation. J. Dyn. Syst. Meas. Control Trans. Asme **107**, 8–16 (1985b)
41. N. Hogan, Impedance control - an approach to manipulation. 3. Applications. J. Dyn. Syst. Meas. Control Trans. Asme **107**, 17–24 (1985c)
42. N. Hogan, Mechanical impedance of single-and multi-articular systems, in *Multiple Muscle Systems: Biomechanics and Movement Organization*, eds. by J. Winters, S. Woo (Springer, New York, 1990)
43. N. Hogan, A general actuator model based on nonlinear equivalent networks. IEEE/ASME Trans. Mechatron. **19**, 1929–1939 (2014)
44. N. Hogan, S.P. Buerger, Impedance and interaction control, in *Robotics and Automation Handbook*, ed by T.R. Kurfess (CRC Press, Boca Raton, FL, 2005)
45. N. Hogan, B.A. Kay, E.D. Fasse, F.A. Mussaivaldi, Haptic illusions - experiments on human manipulation and perception of virtual objects. Cold Spring Harbor Symp. Quant. Biol. **55**, 925–931 (1990)

46. N. Hogan, H.I. Krebs, B. Rohrer, J.J. Palazzolo, L. Dipietro, S.E. Fasoli, J. Stein, R. Hughes, W.R. Frontera, D. Lynch, B.T. Volpe, Motions or muscles? Some behavioral factors underlying robotic assistance of motor recovery. J. Rehab. Res. Dev. **43**, 605–618 (2006)
47. N. Hogan, D. Sternad, Dynamic primitives of motor behavior. Biol. Cybern. **106**, 727–739 (2012)
48. N. Hogan, D. Sternad, Dynamic primitives in the control of locomotion. Front. Comput. Neurosci. **7**, 1–16 (2013)
49. L.A. Hosford, *Development and Testing of an Impedance Controller on an Anthropomorphic Robot for Extreme Environment Operations*, Master of Science, Massachusetts Institute of Technology (2016)
50. D.R. Humphrey, D.J. Reed, Separate cortical systems for control of joint movement and joint stiffness: reciprocal activation and coactivation of antagonist muscles, in *Motor Control Mechanisms in Health and Disease*, ed. by J.E. Desmedt (Raven Press, New York, 1983)
51. G.R. Hunt, Manufacture and use of hook-tools by New Caledonian crows. Nature **379**, 259–251 (1996)
52. A.J. Ijspeert, J. Nakanishi, H. Hoffmann, P. Pastor, S. Schaal, Dynamical movement primitives: learning attractor models for motor behaviors. Neural Comput. **25**, 328–373 (2013)
53. S.H. Johnson-Frey, The neural basis of complex tool use in humans. Trends Cogn. Sci. **8**, 71–78 (2004)
54. D.H. Johnson, Origins of the equivalent circuit concept: the current-source equivalent. Proc. IEEE **91**, 817–821 (2003a)
55. D.H. Johnson, Origins of the equivalent circuit concept: the voltage-source equivalent. Proc. IEEE **91**, 636–640 (2003b)
56. E.R. Kandel, J.H. Schwartz, T.M. Jessell (eds.), *Principles of Neural Science* (McGraw-Hill, New York, 2000)
57. M. Kawato, Internal models for motor control and trajectory planning. Curr. Opin. Neurobiol. **9**, 718–727 (1999)
58. J.A. Kelso, Phase transitions and critical behavior in human bimanual coordination. Am. J. Physiol. Regul. Integr. Comp. Physiol. **246**, R1000–R1004 (1984)
59. J.A.S. Kelso, On the oscillatory basis of movement. Bull. Psychon. Soc. **18**, 49–70 (1981)
60. B. Kenward, A.A.S. Weir, C. Rutz, A. Kacelnik, Behavioral ecology: Tool manufacture by naïve juvenile crows. Nature **433** (2005)
61. H.I. Krebs, M.L. Aisen, B.T. Volpe, N. Hogan, Quantization of continuous arm movements in humans with brain injury. Proc. Natl. Acad. Sci. U.S.A. **96**, 4645–4649 (1999)
62. S. Kuindersma, R. Deits, M. Fallon, A. Valenzuela, H. Dai, F. Permenter, T. Koolen, P. Marion, R. Tedrake, Optimization-based locomotion planning, estimation, and control design for the Atlas humanoid robot. Auton. Robot. **40**, 429–455 (2016)
63. T.M. Kunnapas, An analysis of the "vertical-horizontal illusion". J. Exp. Psychol. **49**, 134–140 (1955)
64. J.R. Lackner, P. Dizio, Rapid adaptation to coriolis force perturbations of arm trajectory. J. Neurophysiol. **72**, 299–313 (1994)
65. H. Lee, P. Ho, M.A. Rastgaar, H.I. Krebs, N. Hogan, Multivariable static ankle mechanical impedance with relaxed muscles. J. Biomech. **44**, 1901–1908 (2011)
66. H. Lee, P. Ho, M.A. Rastgaar, H.I. Krebs, N. Hogan, Multivariable static ankle mechanical impedance with active muscles. IEEE Trans. Neural Syst. Rehab. Eng. **22**, 44–52 (2013)
67. H. Lee, N. Hogan, Time-varying ankle mechanical impedance during human locomotion. IEEE Trans. Neural Syst. Rehab. Eng. (2014)
68. H. Lee, N. Hogan, Energetic passivity of the human ankle joint. IEEE Trans. Neural Syst. Rehab. Eng. (2016)
69. H. Lee, H. Krebs, N. Hogan, Multivariable dynamic ankle mechanical impedance with active muscles. IEEE Trans. Neural Syst. Rehab. Eng. **22**, 971–981 (2014a)
70. H. Lee, H.I. Krebs, N. Hogan, Linear time-varying identification of ankle mechanical impedance during human walking, in *5th Annual Dynamic Systems and Control Conference* (ASME, Fort Lauderdale, Florida, USA, 2012)

71. H. Lee, H.I. Krebs, N. Hogan, Multivariable dynamic ankle mechanical impedance with relaxed muscles. IEEE Trans. Neural Syst. Rehab. Eng. **22**, 1104–1114 (2014b)
72. Y. Li, S.S. GE, Impedance learning for robots interacting with unknown environments. IEEE Trans. Control Syst. Technol. **22** (2014)
73. F.M. Marchetti, S.J. Lederman, The haptic radial-tangential effect: two tests of Wong's 'moments-of-inertia' hypothesis. Bull. Psychon. Soc. **21**, 43–46 (1983)
74. J.C. Maxwell, *A Treatise on Electricity and Magnetism* (1873)
75. H.F. Mayer, Ueber das Ersatzschema der Verstärkerröhre [On equivalent circuits for electronic amplifiers]. Telegraphen- und Fernsprech-Technik **15**, 335–337 (1926)
76. Moog, Moog G761/761 Series Flow Control Servovalves (Moog Inc, 2014)
77. J.M. Morgan, W.W. Milligan, A 1 kHz servohydraulic fatigue testing system, in *Conference on High Cycle Fatigue of Structural Materials*, ed. by Srivatsan, W. O. S. A. T. S. (Warrendale, PA, 1997)
78. W.S. Newman, N. Hogan, High speed robot control and obstacle avoidance using dynamic potential functions, in *IEEE International Conference on Robotics and Automation* (IEEE, New Jersey, 1987)
79. I. Newton, Philosophiæ Naturalis Principia Mathematica (1687)
80. T.R. Nichols, J.C. Houk, Improvement in linearity and regulation of stiffness that results from actions of stretch reflex. J. Neurophysiol. **39**, 119–142 (1976)
81. E.L. Norton, *Design of Finite Networks for Uniform Frequency Characteristic* (Western Electric Company Inc, New York, 1926)
82. J. Ochoa, D. Sternad, N. Hogan, Entrainment of overground human walking to mechanical perturbations at the ankle joint, in *International Conference on Biomedical Robotics and Biomechatronics (BioRob)* (IEEE, Singapore, 2016)
83. L.U. Odhner, L.P. Jentoft, M.R. Claffee, N. Corson, Y. Tenzer, R.R. Ma, M. Buehler, R. Kohout, R.D. Howe, A.M. Dollar, A compliant, underactuated hand for robust manipulation. Int. J. Robot. Res. **33**, 736–752 (2014)
84. N. Paine, S. Oh, L. Sentis, Design and control considerations for high-performance series elastic actuators. IEEE/ASME Trans. Mechatron. **19**, 1080–1091 (2014)
85. R. Plamondon, A.M. Alimi, P. Yergeau, F. Leclerc, Modelling velocity profiles of rapid movements: a comparative study. Biol. Cybern. **69**, 119–128 (1993)
86. R.A. Popat, D.E. Krebs, J. Mansfield, D. Russell, E. Clancy, K.M. Gillbody, N. Hogan, Quantitative assessment of 4 men using above-elbow prosthetic control. Arch. Phys. Med. Rehab. **74**, 720–729 (1993)
87. J. Pratt, J. Carff, S. Drakunov, A. Goswami, Capture point: a step toward humanoid push recovery, in *Humanoids 2006* (IEEE, New Jersey, 2006)
88. D. Rancourt, N. Hogan, Dynamics of pushing. J. Mot. Behav. **33**, 351–362 (2001a)
89. D. Rancourt, N. Hogan, Stability in force-production tasks. J. Mot. Behav. **33**, 193–204 (2001b)
90. D. Rancourt, N. Hogan, The biomechanics of force production, in *Progress in Motor Control: A Multidisciplinary Perspective*, ed by D. Sternad (Springer, Heidelberg, 2009)
91. B. Rohrer, S. Fasoli, H.I. Krebs, B. Volpe, W.R. Frontera, J. Stein, N. Hogan, Submovements grow larger, fewer, and more blended during stroke recovery. Mot. Control **8**, 472–483 (2004)
92. B. Rohrer, N. Hogan, Avoiding spurious submovement decompositions: a globally optimal algorithm. Biol. Cybern. **89**, 190–199 (2003)
93. B. Rohrer, N. Hogan, Avoiding spurious submovement decompositions II: a scattershot algorithm. Biol. Cybern. **94**, 409–414 (2006)
94. R. Ronsse, D. Sternad, P. Lefevre, A computational model for rhythmic and discrete movements in uni- and bimanual coordination. Neural Comput. **21**, 1335–1370 (2009)
95. R. Shadmehr, F.A. Mussa-Ivaldi, Adaptive representation of dynamics during learning of a motor task. J. Neurosci. **14**, 3208–3224 (1994)
96. R.N. Shepard, J. Metzler, Mental rotation of three-dimensional objects. Science **171**, 701–703 (1971)

97. D. Sternad, Towards a unified framework for rhythmic and discrete movements: behavioral, modeling and imaging results, in *Coordination: Neural, Behavioral and Social Dynamics*, eds. by A. Fuchs, V. Jirsa (Springer, New York, 2008)
98. D. Sternad, E.L. Amazeen, M.T. Turvey, Diffusive, synaptic, and synergetic coupling: an evaluation through inphase and antiphase rhythmic movements. J. Mot. Behav. **28**, 255–269 (1996)
99. D. Sternad, D. Collins, M.T. Turvey, The detuning factor in the dynamics of interlimb rhythmic coordination. Biol. Cybern. **73**, 27–35 (1995)
100. D. Sternad, A. de Rugy, T. Pataky, W.J. Dean, Interactions of discrete and rhythmic movements over a wide range of periods. Exp. Brain Res. **147**, 162–174 (2002)
101. D. Sternad, W.J. Dean, Rhythmic and discrete elements in multi-joint coordination. Brain Res. **989**, 152–171 (2003)
102. D. Sternad, W.J. Dean, S. Schaal, Interaction of rhythmic and discrete pattern generators in single-joint movements. Hum. Mov. Sci. **19**, 627–664 (2000)
103. D. Sternad, H. Marino, S.K. Charles, M. Duarte, L. Dipietro, N. Hogan, Transitions between discrete and rhythmic primitives in a unimanual task. Front. Comput. Neurosci. **7** (2013)
104. D. Sternad, M.T. Turvey, R.C. Schmidt, Average phase difference theory and 1:1 phase entrainment in interlimb coordination. Biol. Cybern. **67**, 223–231 (1992)
105. L.C. Thévenin, Sur un nouveau théorème d'électricité dynamique [On a new theorem of dynamic electricity]. Comptes Rendus des Séances de l'Académie des Sciences **97**, 159–161 (1883)
106. W.J. Thompson, *Angular Momentum: An Illustrated Guide to Rotational Symmetries for Physical Systems* (Wiley-Interscience, 1994)
107. B. Vanderborght, A. Albu-Schaeffer, A. Bicchi, E. Burdet, D.G. Caldwell, R. Carloni, M. Catalano, O. Eiberger, W. Friedl, G. Ganesh, M. Garabini, M. Grebenstein, G. Grioli, S. Haddadin, H. Hoppner, A. Jafari, M. Laffranchi, D. Lefeber, F. Petit, S. Stramigioli, N. Tsagarakis, M.V. Damme, R.V. Ham, L.C. Visser, S. Wolf, Variable impedance actuators: a review. Robot. Autonom. Syst. **61**, 1601–1614 (2013)
108. J.M. Wakeling, A.-M. Liphardt, B.M. Nigg, Muscle activity reduces soft-tissue resonance at heel-strike during walking. J. Biomech. **36**, 1761–1769 (2003)
109. J.M. Wakeling, B.M. Nigg, Modification of soft tissue vibrations in the leg by muscular activity. J. Appl. Physiol. **90**, 412–420 (2001)
110. Y. Wang, M. Srinivasan, Stepping in the direction of the fall: the next foot placement can be predicted from current upper body state in steady-state walking. Biol. Lett. **10** (2014)
111. D.M. Wolpert, R.C. Miall, M. Kawato, Internal models in the cerebellum. Trends Cogn. Sci. **2**, 338–347 (1998)
112. G.I. Zahalak, Modeling muscle mechanics (and energetics), in *Multiple Muscle Systems: Biomechanics and Movement Organization*, eds. by J.M. Winters, S.L.-Y. Woo (Springer, New York, 1990)